

RIFE: Real-Time Intermediate Flow Estimation for Video Frame Interpolation

Zhewei Huang¹ Tianyuan Zhang¹ Wen Heng¹ Boxin Shi² Shuchang Zhou¹
¹Megvii Inc ²Peking University

{huangzhewei, zhangtianyuan, hengwen, zsc}@megvii.com, shiboxin@pku.edu.cn

Abstract

We propose RIFE, a Real-time Intermediate Flow Estimation algorithm for Video Frame Interpolation (VFI). Most existing methods first estimate the bi-directional optical flows and then linearly combine them to approximate intermediate flows, leading to artifacts on motion boundaries. RIFE uses a neural network named IFNet that can directly estimate the intermediate flows from images. With the more precise flows and our simplified fusion process, RIFE can improve interpolation quality and have much better speed. Based on our proposed leakage distillation loss, RIFE can be trained in an end-to-end fashion. Experiments demonstrate that our method is significantly faster than existing VFI methods and can achieve state-of-the-art performance on public benchmarks. The code is available at <https://github.com/hzwer/arXiv2020-RIFE>.

1. Introduction

Video Frame Interpolation (VFI) aims to synthesize intermediate frames between two consecutive frames of a video and is widely used to improve the frame rate and enhance visual quality. VFI also supports various applications like slow-motion generation, video compression [31], and training data generation for video motion deblurring [4]. Moreover, VFI algorithms running on high-resolution videos (e.g., 720p, and 1080p) with real-time speed have many more potential applications, such as playing a higher frame rate video on the client’s player, providing video editing services for users with limited computing resources.

VFI is challenging due to the complex, large non-linear motions and illumination changes in the real world. Flow-based VFI algorithms have recently offered a framework to address these challenges and achieved impressive results [17, 22, 35, 2]. Common approaches for these methods involve two steps: 1) warping the input frames according to approximated optical flows and 2) fusing and refining the warped frames using a bunch of Convolutional Neural Net-

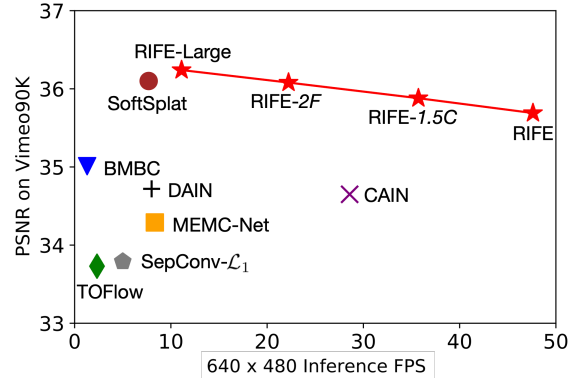


Figure 1: **Speed and accuracy trade-off by adjusting model size parameters C and F .** We compare our models with prior VFI methods including TOFlow [35], SepConv- \mathcal{L}_1 [24], MEMC-Net [3], DAIN [2], CAIN [8], SoftSplat [23] and BMBC [26] on the Vimeo90K testing set.

works (CNNs).

According to the way of warping frames, flow-based VFI algorithms can be classified into forward warping based methods and backward warping based methods. Backward warping is more widely used because forward warping lacks unified and efficient implementation and suffers from conflicts when multiple source pixels are mapped to the same location, which leads to overlapped pixels and holes.

Given the input frames I_0, I_1 , backward warping based methods need to approximate the intermediate flows $F_{t \rightarrow 0}, F_{t \rightarrow 1}$ from the perspective of the frame I_t that we are expected to synthesize. Common practice [17, 34, 2] first computes bi-directional flows from pre-trained off-the-shelf optical flow models, then linearly combines them. This combination, however, will fail on motion boundaries, as there will be different objects in the two frames. Consequently, previous VFI methods share two major drawbacks:

- 1) To solve the artifacts brought by the linear combination of optical flows, previous methods usually need to approximate various representations, e.g., image depth [2], intermediate flow refinement [17]. Coupled with the large complexity in the bi-directional flow estimation,

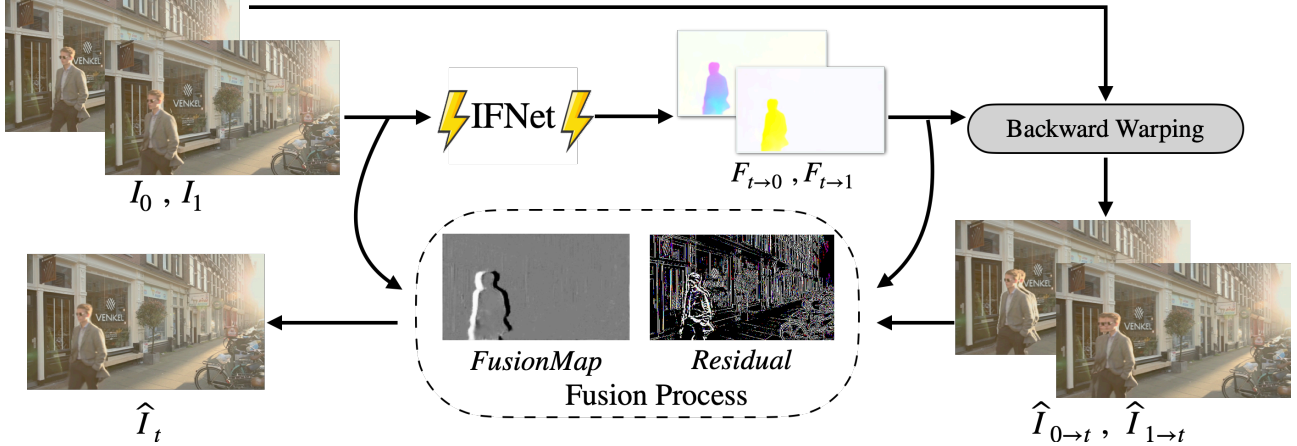


Figure 2: **Overview of RIFE.** Given two input frames I_0, I_1 , we directly feed them into our extremely efficient IFNet to get the intermediate flows $F_{t \rightarrow 0}, F_{t \rightarrow 1}$. Then the fusion process takes the warped frames $\hat{I}_{0 \rightarrow t}, \hat{I}_{1 \rightarrow t}$, intermediate flows $F_{t \rightarrow 0}, F_{t \rightarrow 1}$ and the input frames I_0, I_1 as input. Inside the fusion process, a FusionMap and Residual is firstly estimated, then the warped frames are linearly combined according to the FusionMap, and added with the Residual to get reconstructed intermediate frame \hat{I}_t .

none of these methods can achieve real-time speed.

- 2) Having no direct supervision for the approximated intermediate flows: The intermediate flow estimation process and later refine process is trained with only the final reconstruction loss. There is no other supervision explicitly designed for the flow estimation process, making the whole system hard to converge.

We first develop a specialized and efficient intermediate flow network named IFNet to directly estimate the intermediate flows. IFNet adopts a coarse-to-fine strategy with progressively increased resolutions: it iteratively updates a flow field via successive IFBlocks. Conceptually, according to the iteratively updated flow fields, we move corresponding pixels from two input frames to the same location in a latent intermediate frame. Unlike most previous optical flow models, IFNet does not contain expensive operators like cost volume or pyramid feature warping and simply uses ResNet block [11] as building blocks. This intentional and simple design can benefit from the out-of-the-box efficient implementation of ResNet blocks.

Employing strong intermediate supervision is also found to be important. In fact, when training the IFNet end-to-end with later fusion process using the final reconstruction loss, our method produces worse results than previous methods that used complex pipelines and pre-trained flow models in the intermediate flow estimation process. The picture changes dramatically after we proposed much more advanced supervision to our intermediate flow model, named leakage distillation loss. This novel loss employs an over-powered teacher with access to the intermediate frames during training.

Combining these designs, our algorithm can achieve ex-

cellent results when trained from scratch. We illustrate the speed and accuracy trade-off compared with other methods in Figure 1.

In summary, our contributions are three-fold:

- We design a novel and efficient IFNet to simplify the flow-based VFI methods. IFNet can be trained from scratch and directly approximate the intermediate flows given two input frames.
- We provide effective supervision for the IFNet by proposing an adapted census loss function and a novel leakage distillation loss function, which leads to a more stable convergence and large performance improvement.
- Our proposed RIFE is the first flow-based and real-time VFI algorithm that can process 720p videos at 30FPS. Experiments show that RIFE can achieve impressive performance on public benchmarks.

2. Related Work

We provide a brief overview of the optical flow estimation task, which is the core of most VFI methods. Then, we will review several most related flow-based VFI methods, and cover some inspiring flow-free methods.

2.1. Optical Flow

Optical flow estimation is a long-standing vision task that aims to estimate the per-pixel motion. It provides a useful representation that can be used in lots of downstream tasks like video alignment [5], video editing [33], and video analysis [36]. Since the milestone work of FlowNet [9] based on U-net autoencoder [27], architectures for optical flow model have evolved for several years, yielding

more accurate results while being more efficient, such as FlowNet2 [15], PWCNet [29] and LiteFlowNet [14]. These methods typically adopt an iterative refinement approach and often involve operators like cost volume, pyramidal features, and backward feature warping. Recently Teed *et al.* [30] introduce RAFT, which iteratively updates a flow field through a recurrent unit and achieves a big breakthrough in optical flow estimation. These methods usually use synthetic datasets [9, 15] to perform supervised learning because of the difficulty of optical flow labeling.

Another important direction in this area is unsupervised optical flow estimation learning because of the abundance of video data. Unsupervised methods try to use diverse real data to train an optical flow model that does not suffer from the mismatch between its training data and its test data. The general idea behind all the unsupervised optical flow is that we can use the accurate optical flow between two consecutive images to warp one image to reconstruct the other image’s non-occlusion area. These methods use many constraints such as the smoothness assumption of flow fields [21, 18].

2.2. Video Frame Interpolation

Jiang *et al.* [17] propose the first successful flow-based VFI algorithm named SuperSloMo. It uses the linear combination of the two bi-directional flows estimated by the off-the-shelf optical flow network as an initial approximation of the intermediate flows. Then refine them and predict visibility maps that encode occlusion information. SuperSloMo backward warps the input frames according to refined flow fields and linearly fuse them with the visibility maps to get final results. The whole system is trained with a reconstruction loss in an end-to-end fashion. Later improvements on flow-based VFI algorithms mainly focus on two major components: better flow estimation, better refinement, and fusion of the warped frames. Xu *et al.* [34] exploit four consecutive frames to get the intermediate flow estimation, then fuse the warped frames the same as SuperSloMo. Bao *et al.* [2] improve the flow estimation using a depth-aware flow projection layer, which estimates the intermediate flow as a weighted combination of bidirectional flow using a depth map computed by an off-the-shelf depth estimator, then utilize an adaptive warping layer and frame synthesis network to get the final results.

Along with flow-based methods, flow-free methods have also achieved remarkable progress in recent years. Niklaus *et al.* [25, 22] formulate VFI as a spatially-adaptive convolution whose convolution kernel is generated using a convolution network given the input frames. Choi *et al.* [8] propose an efficient flow-free, fully convolution method named CAIN, which employs the PixelShuffle operator and channel attention to implicitly capture the motion information. Our proposed RIFE achieves comparable results with

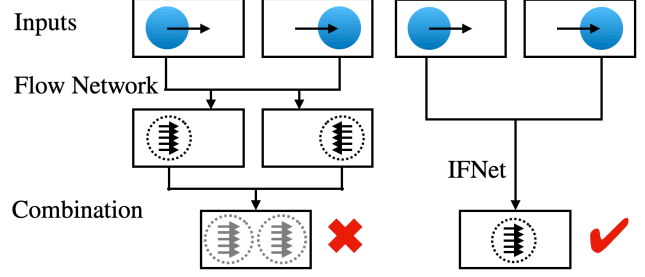


Figure 3: Comparison between previous intermediate flow estimation process (left) and IFNet (right).

state-of-the-art flow-based methods while enjoys the same level of efficiency with the fastest flow-free method.

3. Method

In this section, we first provide an overview of our proposed RIFE. We then describe the efficient design of the major components in RIFE in section 3.2, elaborate on our proposed leakage distillation loss in section 3.3, and explain the training details in section 3.4.

3.1. Pipeline Overview

We illustrate the overview of our proposed RIFE in Figure 2. Given a pair of consecutive RGB frames, I_0, I_1 , our goal is to synthesize an intermediate frame \hat{I}_t at time $t \in (0, 1)$. Previous intermediate flow estimation methods use a bad assumption to directly reverse optical flows [17], which may cause artifacts on motion boundaries, depicted in Figure 3. Our proposed algorithm directly estimate the intermediate flow $F_{t \rightarrow 0}$ by feeding input frames into IFNet. Then we get $F_{t \rightarrow 1}$ using a linear motion assumption:

$$F_{t \rightarrow 1} = -\frac{1-t}{t} F_{t \rightarrow 0}. \quad (1)$$

Note the difference from bi-directional optical flow estimation with the target frame reference. Second, we can get two coarse results $\hat{I}_{0 \rightarrow t}, \hat{I}_{1 \rightarrow t}$ by backward warping the input frames. To remove the artifacts in the warped frames, we feed the input frames, the approximated flow, and warped frames into the fusion process with an encoder-decoder like FusionNet to generate the interpolated frame.

3.2. Efficient Architecture Design

There are two major components in RIFE: (1) Efficient intermediate flow estimation with the **IFNet**. (2) Fusion process of the warped frames using a **FusionNet**. We describe the details of these components in this subsection.

IFNet. We illustrate the detailed architecture of IFNet in Figure 4. The role of our IFNet is to directly and efficiently predict $F_{t \rightarrow 0}$ given two consecutive input frames I_0, I_1 .

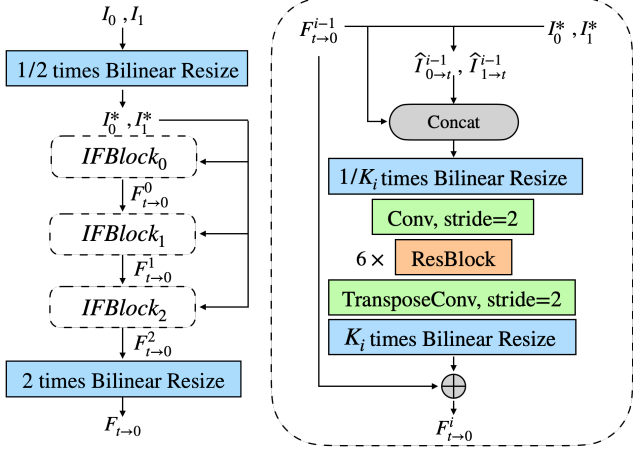


Figure 4: **Structure of IFNet.** **Left:** IFNet is composed of three stacked IFBlocks operating at different resolutions. For model efficiency, we estimate the intermediate flows on the downsampled input frame I_0^*, I_1^* . **Right:** We firstly warp the two input frames based on current approximated flow $F_{t \rightarrow 0}^{i-1}$. Then we feed the warped frames $\hat{I}_{0 \rightarrow t}^{i-1}, \hat{I}_{1 \rightarrow t}^{i-1}$ and $F_{t \rightarrow 0}^{i-1}$ into the IFBlock network to compute a flow residual for the approximation.

Table 1: **Inference time on 720p video.** Standard flow-based VFI methods run the flow estimation network twice to obtain bidirectional optical flows, which takes at least 90 ms. Thus our proposed IFNet achieves a speed of 6–30 times to obtain the intermediate flows.

Method	PWCNet	LiteFlowNet	FlowNet2	IFNet
Runtime	$2 \times 45\text{ms}$	$2 \times 152\text{ms}$	$2 \times 207\text{ms}$	15ms

To handle the large motion encountered in intermediate flow estimation, we employ a coarse-to-fine strategy with gradually increasing resolutions. Specifically, we first compute a rough prediction of the flow on low resolutions, which is believed to capture large motions easier, then iteratively refine the flow fields with gradually increasing resolutions. Following this design, our IFNet has a stacked hourglass structure, where a flow field is iteratively refined via successive IFBlocks operating on increasing resolutions:

$$F_{t \rightarrow 0}^i = F_{t \rightarrow 0}^{i-1} + g^i(F_{t \rightarrow 0}^{i-1}, \hat{I}_{0 \rightarrow t}^{i-1}, \hat{I}_{1 \rightarrow t}^{i-1}), \quad (2)$$

where $F_{t \rightarrow 0}^{i-1}$ denotes the current estimation of the intermediate flow, $\hat{I}_{0 \rightarrow t}^{i-1}$ and $\hat{I}_{1 \rightarrow t}^{i-1}$ denote the warped input frames using previous approximated flow, and g^i represents the i th IFBlock. We use a total of 3 IFBlocks, and each has a resolution parameter, K_i . To keep our design simple, each IFBlock has a feed-forward structure consisting of a down-sampling operator, 6 ResNet blocks, and an up-sampling operator.



Figure 5: **Visual comparison between linearly combined bi-directional flows and results of IFNet.** Our IFNet produces clear and sharp motion boundaries, while linearly combined bi-directional optical flow suffers from overlapped pixels and blurring on motion boundaries.

In Figure 5, we provide visual results of our IFNet and compare them with the linearly combined bi-directional optical flow generated by a pre-trained LiteFlowNet [14]. Our IFNet produces clear and sharp motion boundaries, while linearly combined flow suffers from overlapped pixels and blurring on motion boundaries.

We compare the runtime of the current state-of-the-art optical flow estimation networks [29, 14, 15] and our IFNet in Table 1. Current flow-based models usually need to be run twice to get the bi-directional flow. Thus our intermediate flow estimation process runs around 6 – 30 times faster than previous methods. Thus IFNet provides the possibility of developing a real-time flow-based VFI algorithm.

Fusion process. With the estimated intermediate flows $F_{t \rightarrow 0}, F_{t \rightarrow 1}$, we can get the coarse reconstruction $\hat{I}_{0 \rightarrow t}, \hat{I}_{1 \rightarrow t}$ by performing backward warping on input frames. To reduce the severe artifacts in the warped frames, we perform a refine and fusion process formulated as:

$$\hat{I}_t = M \odot \hat{I}_{0 \rightarrow t} + (1 - M) \odot \hat{I}_{1 \rightarrow t} + \Delta, \quad (3)$$

where M is a soft fusion map used to fuse the two warped frames, Δ is the reconstruction residual term used to refine the details in images, \odot is an element-wise multiplier, and $(0 \leq M, \Delta \leq 1)$.

Following previous work [17, 2, 23], the fusion process includes a context extractor and a FusionNet with an encoder-decoder architecture similar to U-Net. The context extractor and encoder part of the FusionNet have similar architectures, consisting of 4 ResNet blocks with stride as 2. The decoder part in the FusionNet has four transpose convolution layers. We use the sigmoid function to restrict the

outputs of FusionNet.

First, we use the context extractor to extract pyramid contextual features from raw inputs separately. We denote the pyramid contextual feature as C_0 : $\{C_0^1, C_0^2, C_0^3, C_0^4\}$ and C_1 : $\{C_1^1, C_1^2, C_1^3, C_1^4\}$. We perform backward warping on these features using estimated intermediate flows to produce aligned pyramid features, $C_{0 \rightarrow t}$ and $C_{1 \rightarrow t}$. We then feed the warped frames and intermediate flows to the FusionNet to produce the fusion map M and the reconstruction residual Δ , and the output of each block in the encoder part of the FusionNet is concatenated with the corresponding aligned pyramid features before fed into the next block.

Except for the layer that outputs the optical flow residuals, the fusion map, and the reconstruction residual, we use PReLU [10] as the activation function. We use Batch Normalization [16] in IFNet, which is common used to accelerate the convergence. We select a variant of ResNet block named SE-ResNet block [13], which can slightly improve the performance.

3.3. Leakage Distillation for IFNet

Directly approximating the intermediate flow is hard because of no access to the intermediate image and the lack of supervision. To address this problem, during training, we add a leakage distillation loss to our IFNet in which the target is the prediction of an overpowered teacher network who has access to the intermediate frame. Specifically, we feed $\{I_0, I_t^{GT}\}, \{I_t^{GT}, I_1\}$ to a pre-trained optical flow estimation network to get the intermediate flow prediction $\{F_{t \rightarrow 1}^{Leak}, F_{t \rightarrow 0}^{Leak}\}$. And the leakage distillation loss \mathcal{L}_{dis} is defined as follows:

$$\mathcal{L}_{dis} = \|F_{t \rightarrow 0} - F_{t \rightarrow 0}^{Leak}\|_1 + \|F_{t \rightarrow 1} - F_{t \rightarrow 1}^{Leak}\|_1. \quad (4)$$

Our IFNet produces the final flow estimation using an iteratively update procedure, following previous work [30], we apply the leakage distillation loss over the full sequence of predictions.

Our distillation scheme is different from those in semi-supervised learning algorithms [7, 32], where a pre-trained model is used to infer the label of unlabeled data because, with the access of the target intermediate frame I_t^{GT} , our teacher model has a different view of video clip with the student. Conceptually, the overpowered teacher causes a leakage [19] where our flow estimator can have access to the information of the target intermediate frame during training, and in the experiments section, we show that this kind of data (target) leakage is beneficial to the training of our whole system.

3.4. Implement Details

Supervision. Given a pair of consecutive frames, I_0, I_1 , our training loss \mathcal{L} is a linear combination of the reconstruction loss \mathcal{L}_{rec} , census loss [21] \mathcal{L}_{cen} and leakage distillation

loss \mathcal{L}_{dis} as defined in section 3.3:

$$\mathcal{L} = \mathcal{L}_{rec} + \lambda_c \mathcal{L}_{cen} + \lambda_d \mathcal{L}_{dis}, \quad (5)$$

where we set $\lambda_c = 1$ and $\lambda_d = 0.01$.

The reconstruction loss \mathcal{L}_{rec} models the reconstruction quality of the intermediate frame. We denote the synthesized frame by $\hat{\mathbf{I}}_t$ and the ground-truth frame by \mathbf{I}_t^{GT} . The reconstruction loss has the formulation of :

$$\mathcal{L}_{rec} = \sum_{\mathbf{x}} \rho \left(\hat{\mathbf{I}}_t(\mathbf{x}) - \mathbf{I}_t^{GT}(\mathbf{x}) \right), \quad (6)$$

where $\rho(x) = \sqrt{x^2 + \epsilon^2}$ is the Charbonnier penalty function [6]. We set the constant ϵ to 10^{-6} .

As the brightness constancy constraint is often violated in realistic situations, census loss is widely used in unsupervised optical flow estimation [18] methods to address the illumination changes. We adopt the census loss in our framework to robustly handle the illumination changes between consecutive frames. The census loss is defined as the soft Hamming distance on census-transformed [37] image patches. We optimize the census loss between census-transformed $\hat{\mathbf{I}}_t$ and \mathbf{I}_t^{GT} with the width of patches as 9.

Training dataset. We use the Vimeo90K dataset [35] to train our model. The Vimeo90K dataset has 51,312 triplets for training, where each triplet contains three consecutive video frames with a resolution of 256×448 . We train our network to predict the middle frame (*i.e.*, $t = 0.5$) of each triplet. We randomly augment the training data by horizontal and vertical flipping and reversing the triplet's temporal order during training.

Training strategy. We train our system from scratch on the Vimeo90K training set. A LiteFlowNet [14] pre-trained on the FlyingChairs [9] dataset is used as the overpowered teacher in the leakage distillation.

Our model is optimized by AdamW [20] with weight decay 10^{-5} for 300 epochs on the Vimeo90K training set. The training is based on 224×224 patches and uses a batch size of 64. We gradually reduce the learning rate from 5×10^{-4} to 0 using cosine annealing during the whole training process. Our pipeline is implemented in PyTorch. We train RIFE on four NVIDIA TITAN X (Pascal) GPUs, which takes about 15 hours to converge. The preprocess needs 2 hours in one GPU, and different models can use the same preprocess results.

4. Experiments

In this section, we conduct several experiments to validate our method. We first introduce the benchmarks for evaluation. Then we provide variants of our models with

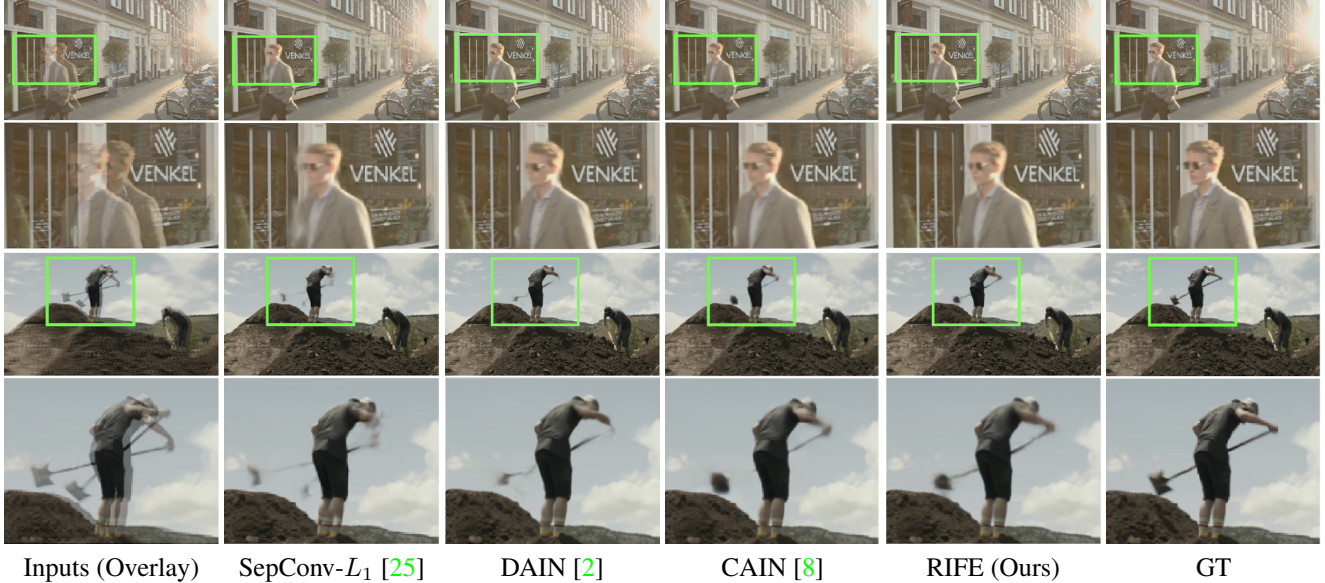


Figure 6: **Qualitative comparison on Vimeo90K testing set.** We cut out the moving objects according to the green boxes and zoom in the results. While other methods cause various artifacts, our method produces best effects on the moving objects.

Table 2: **Quantitative comparisons on the UCF101, Vimeo90K, Middlebury OTHER set, and HD benchmarks.** The numbers in **red** and **blue** represent the best and second-best performance. We report the interpolation runtime for a single 640×480 video frame. The following works are sorted by publication time.

Method	# Parameters (Million)	Runtime (ms)	UCF101 [28]		Vimeo90K [35]		Middlebury [1]	HD [3]
			PSNR	SSIM	PSNR	SSIM	IE	PSNR
TOFlow [35]	1.1	430	34.58	0.967	33.73	0.968	2.15	29.37
SepConv- \mathcal{L}_1 [24]	21.6	200	34.78	0.967	33.79	0.970	2.27	30.87
MEMC-Net [3]	70.3	121	35.01	0.968	34.40	0.970	2.12	31.60
DAIN [2]	24.0	125	35.00	0.968	34.71	0.976	2.04	31.64
CAIN [8]	42.8	32*	34.91	0.969	34.65	0.973	2.28	30.70*
SoftSplat [23]	7.7	135	35.39	0.970	36.10	0.980	-	-
BMBC [26]	11.0	770	35.15	0.969	35.01	0.976	-	-
RIFE (Ours)	10.4	21	35.14	0.969	35.69	0.978	2.05	32.04
RIFE-Large (Ours)	22.9	90	35.33	0.970	36.24	0.981	1.98	32.18

*: use officially released models to produce results

different computational costs to meet different needs in section 4.2. We compare our models with representative state-of-the-art methods, both quantitatively and visually, in section 4.3. An ablation study in section 4.4 is carried out to analyze our design of IFNet and the proposed leakage distillation loss. Finally, we show the capability of generating multiple frames using our models in section 4.5.

4.1. Benchmarks and Evaluation Metrics

We evaluate our model on four benchmarks, including Middlebury [1], UCF101 [28], Vimeo90K [35] and HD [3] benchmark. Following previous work, we train our models on the Vimeo90K training dataset and directly test it on all

these benchmarks.

Middlebury. The Middlebury benchmark is widely used to evaluate VFI methods. The image resolution in this dataset is around 640×480 . There are two sets of Middlebury benchmark. We report the average interpolation error (IE) of the OTHER set.

Vimeo90K. There are 3,782 triplets in the Vimeo90K testing set [35]. The image resolution in this dataset is 448×256 .

UCF101. The UCF101 dataset [28] contains videos with a large variety of human actions. There are 379 triplets with a resolution of 256×256 .

HD. Bao *et al.* [3] collect 11 high-resolution videos for

Table 3: **Increase model complexity by adjusting model size parameters.** C denotes the multiplier for the number of channels, and F denotes the resolution multiplier. $2F$ represents removing the first downsampling layer of IFNet and the first one of FusionNet. The parameter setting of RIFE-Large is $1.5C2F$.

Scale Setting	RIFE	$1.5C$	$2F$	RIFE-Large
UCF101 PSNR	35.14	35.26	35.32	35.33
Vimeo90K PSNR	35.69	35.88	36.08	36.24
Middlebury IE	2.03	2.03	1.99	1.98
HD PSNR	32.04	32.13	31.96	32.18
# Parameters*	10.4M	22.9M	10.4M	22.9M
Runtime*	36ms	65ms	126ms	196ms
Complexity*	83G	185G	322G	724G

*: measure the whole algorithm on 720p videos

evaluation. The HD dataset consists of four 1080p, three 720p and four 1280×544 videos. The motions in this benchmark are larger than other benchmarks.

We measure the peak signal-to-noise ratio (PSNR) and structural similarity (SSIM) for quantitative evaluation.

4.2. Model Scaling

We provide several models with different computation cost and performance to meet different needs by model scaling. We introduce two hyper-parameters following [12]: width multiplier and resolution multiplier. Upon our base model RIFE, we apply a width multiplier on the number of channels uniformly at each layer. Choosing the width multiplier to 1.5 produces a model named RIFE- $1.5C$. Meanwhile, we can remove a downsample layer from the headers of IFNet and FusionNet, which doubles the feature map’s width and height that produces a model named RIFE- $2F$. Together, we can combine these two modifications to produce a model named RIFE-Large ($1.5C2F$). The performance and runtime for these models is reported in Table 3 and depicted in Figure 1. We confirm that our model design is flexible, and increasing model capacity can effectively improve model performance.

4.3. Comparisons with Previous Methods

We compare RIFE with representative state-of-the-art models including

- **Backward warping based methods:** TOFlow [35], MEMC-Net [3], DAIN [2], BMBC [26].
- **Forward warping based methods:** SoftSplat [23].
- **Flow-free methods:** SepConv [25], CAIN [8].

We report the performance metric on benchmarks mentioned above and running speed measured on an NVIDIA TITAN X (Pascal) GPU with an input resolution of 640×480 in Table 2. Our base model RIFE runs considerably

Table 4: **Different scale settings of the IFBlocks.** Our IFNet adopt the (4, 2, 1) setting. The (1, 1, 1) combination yields better performance only on UCF101 whose videos have a limited resolution of 256×256 .

K_1, K_2, K_3	4, 2, 1	1, 1, 1	4, 4, 4	2, 1
UCF101 PSNR	35.14	35.21	29.35	35.20
Vimeo90K PSNR	35.69	35.64	35.20	35.60
Middlebury IE	2.03	2.04	2.28	2.09
HD PSNR	32.04	32.00	31.95	31.84
#Parameters*	6.3M	1.4M	20.8M	2.3M
Runtime*	15ms	17ms	13ms	12ms
Complexity*	44.0 GFlops			

*: measure the IFNet part on 720p videos

Table 5: **Different loss function settings.** Removing the leakage distillation loss function results in large performance drop, especially on high-resolution benchmarks.

Reconstruction Loss	✓	✓	✓	✓
Census Loss	✓		✓	
Distillation Loss	✓	✓		
UCF101 PSNR	35.14	35.12	35.13	35.06
Vimeo90K PSNR	35.69	35.48	35.14	34.88
Middlebury IE	2.03	2.08	2.38	2.45
HD PSNR	32.04	31.89	31.12	30.93

faster than all compared methods with comparable performance. A larger version of our model, namely RIFE-Large, runs 30% faster than the previous state-of-the-art method SoftSplat [23] with better performance on several benchmarks. We provide a visual comparison on video clips with large motions from the Vimeo90K testing set. We show the results in Figure 6, where SepConv- L_1 and DAIN produce ghosting artifacts, and CAIN causes missing-parts artifacts in the shovel. Overall, our method can produce more reliable results.

4.4. Ablation Study

Ablation on the design of IFNet. To validate the effectiveness of the coarse-to-fine procedure with gradually increasing resolution, we perform a small ablation study on IFNet. We construct three models with the same architecture with our IFNet except for the combination of resolution parameters for each IFBlock. We compare the performance and runtime of these models in Table 4.

Ablation on the loss functions. We perform an ablation study to analyze the contributions of the proposed leakage distillation loss function and the adopted census loss function. We list the results of training our models under different loss function settings in Table 5. We confirm that



Figure 7: **Interpolating multiple frames on the Vimeo90K testing dataset by applying RIFE recursively.** We cut out the moving objects according to the green boxes and zoom in the results. RIFE provides smooth and continuous motions.

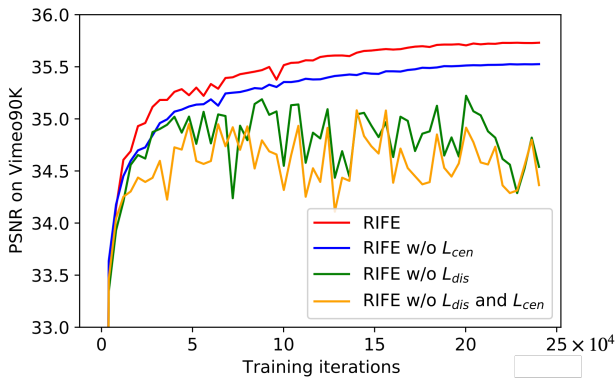


Figure 8: **Different loss function settings.** We evaluate RIFE on the Vimeo90K testing set for every 5 training epochs. Removing the leakage distillation loss function leads to unstable convergence and performance degradation.

these two loss functions can improve the performance of RIFE. We also depict the PSNR curves on the Vimeo90K testing dataset during model training in Figure 8. We can observe that removing the leakage distillation loss function leads to extremely unstable convergence and severe performance degradation, and the adopted census loss function can slightly improve the performance. From Table 5, removing the leakage distillation loss function leads to large

model performance drop on Vimeo90K and HD benchmarks with large resolution. This phenomenon is likely because our proposed leakage distillation loss function dramatically improves the model capability to capture larger motions.

4.5. Generating Multiple Frames

To interpolate multiple intermediate frames at different time $t \in (0, 1)$, we can apply RIFE recursively. Specifically, given any two consecutive input frames I_0, I_1 , we apply RIFE once to get intermediate frame $\hat{I}_{0.5}$ at $t = 0.5$, then we feed I_0 and $\hat{I}_{0.5}$ to get $\hat{I}_{0.25}$, and we can repeat this process recursively to get the $8\times, 16\times$ results.

To demonstrate this ability, we provide the visual results for $2\times, 4\times, 8\times$ settings on images with large motions from the Vimeo90K testing set in Figure 7. We observe that RIFE successfully produces smooth and continuous motions.

5. Conclusion

In this paper, we develop an efficient and flexible algorithm for VFI, named RIFE. Unlike common flow-based VFI methods, RIFE produces the intermediate flows using an efficient CNN. With the more precise flows and our simplified fusion process, RIFE can effectively process videos of different resolutions, successfully interpolate multiple frames between two input frames, and surpass existing methods on public benchmarks.

References

- [1] baker2011database. A database and evaluation methodology for optical flow. In *International Journal of Computer Vision (IJCV)*, 2011. 6
- [2] Wenbo Bao, Wei-Sheng Lai, Chao Ma, Xiaoyun Zhang, Zhiyong Gao, and Ming-Hsuan Yang. Depth-aware video frame interpolation. In *Proceedings of the IEEE Conference on Computer Vision and Pattern Recognition (CVPR)*, 2019. 1, 3, 4, 6, 7
- [3] Wenbo Bao, Wei-Sheng Lai, Xiaoyun Zhang, Zhiyong Gao, and Ming-Hsuan Yang. Memc-net: Motion estimation and motion compensation driven neural network for video interpolation and enhancement. *IEEE Transactions on Pattern Analysis and Machine Intelligence (IEEE TPAMI)*, 2018. 1, 6, 7
- [4] Behzad Bozorgtabar, Mohammad Saeed Rad, Hazım Kemal Ekenel, and Jean-Philippe Thiran. Learn to synthesize and synthesize to learn. *Computer Vision and Image Understanding*, 185:1–11, 2019. 1
- [5] Jose Caballero, Christian Ledig, Andrew Aitken, Alejandro Acosta, Johannes Totz, Zehan Wang, and Wenzhe Shi. Real-time video super-resolution with spatio-temporal networks and motion compensation. In *Proceedings of the IEEE Conference on Computer Vision and Pattern Recognition (CVPR)*, 2017. 2
- [6] Pierre Charbonnier, Laure Blanc-Feraud, Gilles Aubert, and Michel Barlaud. Two deterministic half-quadratic regularization algorithms for computed imaging. In *Proceedings of 1st International Conference on Image Processing (ICIP)*, 1994. 5
- [7] Ting Chen, Simon Kornblith, Kevin Swersky, Mohammad Norouzi, and Geoffrey Hinton. Big self-supervised models are strong semi-supervised learners. *arXiv preprint arXiv:2006.10029*, 2020. 5
- [8] Myungsub Choi, Heewon Kim, Bohyung Han, Ning Xu, and Kyoung Mu Lee. Channel attention is all you need for video frame interpolation. In *Proceedings of the Association for the Advancement of Artificial Intelligence (AAAI)*, 2020. 1, 3, 6, 7
- [9] Alexey Dosovitskiy, Philipp Fischer, Eddy Ilg, Philip Hausser, Caner Hazirbas, Vladimir Golkov, Patrick Van Der Smagt, Daniel Cremers, and Thomas Brox. FlowNet: Learning optical flow with convolutional networks. In *Proceedings of the IEEE International Conference on Computer Vision (ICCV)*, 2015. 2, 3, 5
- [10] Kaiming He, Xiangyu Zhang, Shaoqing Ren, and Jian Sun. Delving deep into rectifiers: Surpassing human-level performance on imagenet classification. In *Proceedings of the IEEE International Conference on Computer Vision (ICCV)*, 2015. 5
- [11] Kaiming He, Xiangyu Zhang, Shaoqing Ren, and Jian Sun. Deep residual learning for image recognition. In *Proceedings of the IEEE Conference on Computer Vision and Pattern Recognition (CVPR)*, 2016. 2
- [12] Andrew G Howard, Menglong Zhu, Bo Chen, Dmitry Kalenichenko, Weijun Wang, Tobias Weyand, Marco Andreetto, and Hartwig Adam. Mobilenets: Efficient convolutional neural networks for mobile vision applications. *arXiv preprint arXiv:1704.04861*, 2017. 7
- [13] Jie Hu, Li Shen, and Gang Sun. Squeeze-and-excitation networks. In *Proceedings of the IEEE conference on computer vision and pattern recognition (CVPR)*, 2018. 5
- [14] Tak-Wai Hui, Xiaoou Tang, and Chen Change Loy. Lite-flownet: A lightweight convolutional neural network for optical flow estimation. In *Proceedings of the IEEE Conference on Computer Vision and Pattern Recognition (CVPR)*, 2018. 3, 4, 5
- [15] Eddy Ilg, Nikolaus Mayer, Tonmoy Saikia, Margret Keuper, Alexey Dosovitskiy, and Thomas Brox. Flownet 2.0: Evolution of optical flow estimation with deep networks. In *Proceedings of the IEEE Conference on Computer Vision and Pattern Recognition (CVPR)*, 2017. 3, 4
- [16] Sergey Ioffe and Christian Szegedy. Batch normalization: Accelerating deep network training by reducing internal covariate shift. *arXiv preprint arXiv:1502.03167*, 2015. 5
- [17] Huaizu Jiang, Deqing Sun, Varun Jampani, Ming-Hsuan Yang, Erik Learned-Miller, and Jan Kautz. Super slo-mo: High quality estimation of multiple intermediate frames for video interpolation. In *Proceedings of the IEEE Conference on Computer Vision and Pattern Recognition (CVPR)*, 2018. 1, 3, 4
- [18] Rico Jonschkowski, Austin Stone, Jonathan T Barron, Ariel Gordon, Kurt Konolige, and Anelia Angelova. What matters in unsupervised optical flow. In *Proceedings of the European Conference on Computer Vision (ECCV)*, 2020. 3, 5
- [19] Shachar Kaufman, Saharon Rosset, Claudia Perlich, and Ori Stitelman. Leakage in data mining: Formulation, detection, and avoidance. *ACM Transactions on Knowledge Discovery from Data (TKDD)*, 6(4):1–21, 2012. 5
- [20] Ilya Loshchilov and Frank Hutter. Fixing weight decay regularization in adam. 2018. 5
- [21] Simon Meister, Junhwa Hur, and Stefan Roth. UnFlow: Unsupervised learning of optical flow with a bidirectional census loss. In *Proceedings of the Association for the Advancement of Artificial Intelligence (AAAI)*, 2018. 3, 5
- [22] Simon Niklaus and Feng Liu. Context-aware synthesis for video frame interpolation. In *Proceedings of the IEEE Conference on Computer Vision and Pattern Recognition (CVPR)*, 2018. 1, 3
- [23] Simon Niklaus and Feng Liu. Softmax splatting for video frame interpolation. In *Proceedings of the IEEE Conference on Computer Vision and Pattern Recognition (CVPR)*, 2020. 1, 4, 6, 7
- [24] Simon Niklaus, Long Mai, and Feng Liu. Video frame interpolation via adaptive separable convolution. In *Proceedings of the IEEE International Conference on Computer Vision (ICCV)*, 2017. 1, 6
- [25] Simon Niklaus, Long Mai, and Feng Liu. Video frame interpolation via adaptive separable convolution. In *Proceedings of the IEEE International Conference on Computer Vision (ICCV)*, 2017. 3, 6, 7
- [26] Junheum Park, Keunsoo Ko, Chul Lee, and Chang-Su Kim. Bmbc: Bilateral motion estimation with bilateral cost volume for video interpolation. In *Proceedings of the European Conference on Computer Vision (ECCV)*, 2020. 1, 6, 7

- [27] Olaf Ronneberger, Philipp Fischer, and Thomas Brox. U-net: Convolutional networks for biomedical image segmentation. In *International Conference on Medical image computing and computer-assisted intervention (MICCAI)*, 2015. 2
- [28] Khurram Soomro, Amir Roshan Zamir, and Mubarak Shah. UCF101: A dataset of 101 human actions classes from videos in the wild. *CoRR*, abs/1212.0402, 2012. 6
- [29] Deqing Sun, Xiaodong Yang, Ming-Yu Liu, and Jan Kautz. Pwc-net: Cnns for optical flow using pyramid, warping, and cost volume. In *Proceedings of the IEEE Conference on Computer Vision and Pattern Recognition (CVPR)*, 2018. 3, 4
- [30] Zachary Teed and Jia Deng. Raft: Recurrent all-pairs field transforms for optical flow. In *Proceedings of the European Conference on Computer Vision (ECCV)*, 2020. 3, 5
- [31] Chao-Yuan Wu, Nayan Singhal, and Philipp Krahenbuhl. Video compression through image interpolation. In *Proceedings of the European Conference on Computer Vision (ECCV)*, 2018. 1
- [32] Qizhe Xie, Minh-Thang Luong, Eduard Hovy, and Quoc V Le. Self-training with noisy student improves imagenet classification. In *Proceedings of the IEEE Conference on Computer Vision and Pattern Recognition (CVPR)*, 2020. 5
- [33] Rui Xu, Xiaoxiao Li, Bolei Zhou, and Chen Change Loy. Deep flow-guided video inpainting. In *Proceedings of the IEEE Conference on Computer Vision and Pattern Recognition (CVPR)*, June 2019. 2
- [34] Xiangyu Xu, Li Siyao, Wenxiu Sun, Qian Yin, and Ming-Hsuan Yang. Quadratic video interpolation. In *Advances in Neural Information Processing Systems (NIPS)*, 2019. 1, 3
- [35] Tianfan Xue, Baian Chen, Jiajun Wu, Donglai Wei, and William T Freeman. Video enhancement with task-oriented flow. In *International Journal of Computer Vision (IJCV)*, 2019. 1, 5, 6, 7
- [36] Joe Yue-Hei Ng, Matthew Hausknecht, Sudheendra Vijayanarasimhan, Oriol Vinyals, Rajat Monga, and George Toderici. Beyond short snippets: Deep networks for video classification. In *Proceedings of the IEEE Conference on Computer Vision and Pattern Recognition (CVPR)*, 2015. 2
- [37] Ramin Zabih and John Woodfill. Non-parametric local transforms for computing visual correspondence. In *Proceedings of the European Conference on Computer Vision (ECCV)*, 1994. 5